Geoscience Letters

RESEARCH LETTER

Open Access

Evaluation of different machine learning models and novel deep learning-based algorithm for landslide susceptibility mapping

Tingyu Zhang[1,2], Yanan Li[1,2], Tao Wang[3], Huanyuan Wang[4*], Tianqing Chen[1,2], Zenghui Sun[1,2], Dan Luo[3], Chao Li[3] and Ling Han[4]

Abstract

The losses and damage caused by landslide are countless in the world every year. However, the existing approaches of landslide susceptibility mapping cannot fully meet the requirement of landslide prevention, and further excavation and innovation are also needed. Therefore, the main aim of this study is to develop a novel deep learning model namely landslide net (LSNet) to assess the landslide susceptibility in Hanyin County, China, meanwhile, support vector machine model (SVM) and kernel logistic regression model (KLR) were employed as reference model. The inventory map was generated based on 259 landslides, the training dataset and validation dataset were, respectively, prepared using 70% landslides and the remaining 30% landslides. The variance inflation factor (VIF) was applied to optimize each landslide predisposing factor. Three benchmark indices were used to evaluate the result of susceptibility mapping and area under receiver operating characteristics curve (AUROC) was used to compare the models. Result demonstrated that although the processing speed of LSNet model is the slowest, it still significantly outperformed its corresponding benchmark models with validation dataset, and has the highest accuracy (0.950), precision (0.951), F1 (0.951) and AUROC (0.941), which reflected excellent predictive ability in some degree. The achievements obtained in this study can improve the rapid response capability of landslide prevention for Hanyin County.

Keyword: Landslide susceptibility, Deep learning, Kernel logistic regression, Support vector machine, Evaluation

Instruction

Landslide is defined as the special geological phenomenon that is threatening to mankind triggered by human activities or natural factors. Under the dual background of human activities and natural transmutations, the occurrence rate of landslides in the world increased rapidly (Sun et al. 2020). Depending on the latest statistical report of Ministry of Natural Resources of China (http://www.mnr.gov.cn/), in total 6,181 geological hazards occurred in 2019, during that year, 211 people were killed and direct economic loss valued at 397 million dollars. Due to complex terrain, tectonic development and human activities, there are more than 230,000 potential geological hazards in China and landslides account for 53.50% of it. Therefore, the prevention of landslide development in China is crucial. In the face of increasingly serious landslide threats, the development of disaster prevention and mitigation work can effectively reduce the threat posed by landslides. In order to plan and construct the city safely and effectively, and to carry out the work of disaster prevention and mitigation successfully, it is necessary to quantitatively assess the landslide susceptibility on the regional scale.

Over the past years, various techniques and methods for forecasting the landslides have been applied to landslide susceptibility assessment (LSA). At first, with the help of historical landslide data and the geological

*Correspondence: whysxdj2021@163.com

[4] School of Land Engineering, Chang'an University, Xi'ani 710054, Shaanx, China
Full list of author information is available at the end of the article

environment background, the scope of landslide prediction was directly delineated, but this method relies heavily on experience, resulting in low reliability of the results (Guzzetti et al. 2012; Youssef and Pourghasemi 2021). With the development of geographic information system (GIS) and satellite remote sensing technology within each subject area, the more commonly used solutions can be summarized as a few steps. The first step of LSA is to collect the development characteristics and spatial distribution features of historical and hidden danger landslides (Pradhan and Lee 2010). Then the predisposing factors of landslide occurrence are selected from the geological and environment background. Subsequently, the linear or non-linear mapping relationship between predisposing factors and the degree of landslide susceptibility is analyzed by using evaluation model (qualitative or quantitative), and the contribution rate of each landslide predisposing factor is determined. In the end, some techniques of analysis and comparison are used to choose the suitable model for the study area (Carrara et al. 1995).

In principle, the evaluation models used in LSA could be crude categorized as two classes: statistical model and machine learning model. Usually, the statistical models were conjugated to GIS for spatial variety prediction of landslide disaster. The frequently used models are index of entropy (IOE) (Constantin et al. 2011; Youssef et al. 2015), analytical hierarchy process (AHP) (Kayastha et al. 2013), frequency ratio (FR) (Umar et al. 2014; Razavizadeh et al. 2017), certainty factor (CF) (Fan et al. 2017; Li and Zhang 2017), logistic regression (LR) (Pourghasemi et al. 2013; Aditian et al. 2018) and evidential belief function (EBF) (Carranza 2015; Li and Wang 2019). As the predictive ability of statistical model is still deficient and with the development of information technology, machine learning models could be a better alternative to solve the susceptibility assessment problem, such as artificial neural networks (ANN) (Aditian et al. 2018; Polykretis and Chalkias 2018; SOMA et al. 2019), support vector machines (SVM) (Bui et al. 2016; Pandey and Pourghasemi 2020), adaptive neuro-fuzzy inference systems (ANFIS)(Aghdam et al. 2017), decision trees (DT) (Pham et al. 2016), fuzzy logic (FL) (Saadoud et al. 2018) and multivariate adaptive regression spines (MARS) (Conoscenti et al. 2014). Due to data quality, factor selection, model parameter adjustment and other factors, some low accuracy, over fitting, and under fitting problems often appear (Bui et al. 2018). In order to solve these problems, hybrid model was developed in recent years, such as reduced error pruning trees (REPT) (Pham et al. 2019), kernel logistic regression model integrated with fractal dimension ($KLR_{box\text{-}counting}$) (Zhang et al. 2019), support vector regression model integrated with gray wolf optimization algorithm (SVR-GWO) (Balogun et al. 2021), adaptive neuro-fuzzy inference system model integrated with satin bowerbird optimizer algorithms (ANFIS-SBO) (Chen et al. 2021). However, these machine learning models still cannot avoid some disadvantages, for example, (1) It still requires a lot of prior knowledge and erection; (2) the existing network cannot fully extract potential landslide features; (3) the models are sensitive to missing data, and prone to fall into local optima.

Compared with machine learning, deep learning (DL) does not need to manually construct and select feature layers when dealing with object features, and at the same time, deep learning accepts a larger sample size, which is gradually applied in various fields. For example, Panahi (2020) used convolutional neural networks and recurrent neural networks to predict the probability of flash flood (Panahi et al. 2020); Kumar (2020) used deep learning model to complete the prediction of ground water depth (Kumar et al. 2020); Benzekri (2020) employed the deep learning model to construct an early forest fire detection system (Benzekri et al. 2020). In general, DL model performed a satisfactory ability of classification and regression. The main reason is that DL is completely a data-driven feature learning method, and has multi-level non-linear operations, which can abstractly represent classification features from a large amount of data, and combines gradient transfer method to optimize its end-to-end network structure (Zhu et al. 2020). Recently, more and more DL models have been successively applied in the field of LSA (Xiao et al. 2018; Huang et al. 2020; Li et al. 2021), among the different DL models, convolutional neural network (CNN) plays a significant role in landslide recognition and prediction, for example, Wang (2019) applied three novel CNN architectures in LSA, which achieved higher prediction accuracy than conventional methods (Wang et al. 2019); Sameen (2020) developed a DL-based technique for LSA through a 1-dimensional CNN, which performed better than ANN and SVM (Sameen et al. 2020); Fang et al. (2021) constructed four heterogeneous ensemble-learning techniques combining with CNN, RNN, SVM, and LR, the final results also showed that the DL model performed best (Fang et al. 2021).

However, these previous studies have some shortcomings, for example, in the process of building DL model, each convolutional layer will bring different prediction effects, the construction of multi-channel networks is ignored for landslide predisposing factor. Moreover, due to China's vast territory and diverse geological environment, there is still a lack of databases and studies related to landslides, and more reasonable, reliable and more accurate DL models still need to be explored.

Therefore, this study proposed a novel deep learning network named LSNet composed of multiple convolutional layers to predict the landslide susceptibility in Hanyin County, Shaanxi Province, China. The patches of landslide predisposing factor maps were used as the input data to train the LSNet, meanwhile the LSI was regarded as the output to predict the landslide susceptibility. In addition, the support vector machine model (SVM) and kernel logistic regression model (KLR) were employed to compare with LSNet. The primary difference here between this study and the literature mentioned is that approaches existed in this paper are seldom used and compared in landslide susceptibility assessment, especially LSNet and KLR. Another point is that the three models were first applied in Hanyin County and LSNet with multiple channels was established combined with the data structure representing the landslide, with the aim to improve the accuracy of LSA in the study area. Finally, all the results may help the government to make efficient decisions about landslide prevention and provide prevention references for landslide risk.

Sample description of study area

Hanyin County belongs to the hilly area in southern Shaanxi Province, the geographical coordinates are 32°68'-33°09'north latitude and 108°11'-108°44'east longitude (Fig. 1). The study area is about 51 km wide from east to west, 58 km long from north to south, and covers an area of about 1347 Km^2. The climate type of study area is continental tropical monsoon climate and the temperature varies greatly. According to the local meteorological statistics, the mean annual precipitation in the past 50 years is about 920 mm, and the rainfall in the northern region is significantly less than that in the southern region. The water resources in the study area are very abundant, and there are 4 rivers in total, all of which belong to Yangtze River system. There are three types of groundwater in the study area, including loose rock pore water, carbonate fissure water, and bedrock fissure water.

The geomorphology of study area is dominated by low and middle mountains, with valleys, hills and basins, and the area of mountains accounts for 87%. The exposed strata and main lithology in the study area are shown in Table 1. Since the geotectonic location of the study area is located in the core zone of the Qinling microplate, there are many faults and folds in this area. In fact, there are a total of 5 faults that have been proven. Besides, according to the historical records, there have been 16 earthquakes in the study area, with an average magnitude of 4, but these earthquakes did not cause major damage.

Data preparation

Landslide inventory

Before carrying out the LSA, it is critical to verify about the information of landslides in the study area. Landslide inventory is to integration of landslide boundaries, locations, types and so on, which is the subsequent basis of data analysis and model construction. Based on the historical landslide data (SBGMR 1989; PRC 2020), remote sensing image (Cloud 2020), literatures (Liu and Huang 2006) and field survey, a total of 267 landslide locations were identified from 1989–2020 as the reference. These landslide locations were then imported into the GF-2 remote sensing images to delineated landslide boundary in ArcGIS software. In order to generate the landslide inventory map of study area (Fig. 1), all landslide boundaries were converted into polygons and resampled with the resolution of 30 m × 30 m. Figure 2 shows the preparation process of landslide inventory map.

Data preparation

In order to prepare the input dataset for model construction, 267 landslide samples were separated into two parts according to the ratio of 7/3 (Zhao and Chen 2020). Among them, 187 landslide samples were used as the training dataset to train the model, and the remaining 80 landslide samples were applied as the validation dataset to finish the validation purpose.

Analysis and quantification of landslide predisposing factors

There are no fixed guidelines for selecting the predisposing factors for LSA. After the comprehensive analysis of regional geo-environment characteristics and previous researches (Zhou and Fang 2015; Wang et al. 2020; Wu et al. 2020), we proposed altitude, slope angle, slope aspect, normalized difference vegetation index (NDVI), distance to rivers, distance to roads, distance to faults, mean annual precipitation (MAP) and lithology as the landslide predisposing factors.

Among them, altitude, slope angle, slope aspect are commonly used terrain factors, which can describe the influence of terrain on landslide with multi-dimension. For instance, altitude can affect the topographic properties, vegetation distribution and temperature differences at different heights. Slope angle is regarded as one major impact factor affecting instability and deformation of landslides, for example, the larger the slope angle, the less stable the slope is.

NDVI is a commonly used to indicate the vegetation coverage condition and it ranges from -1 to 1. Negative value expresses that there is water, snow and cloud

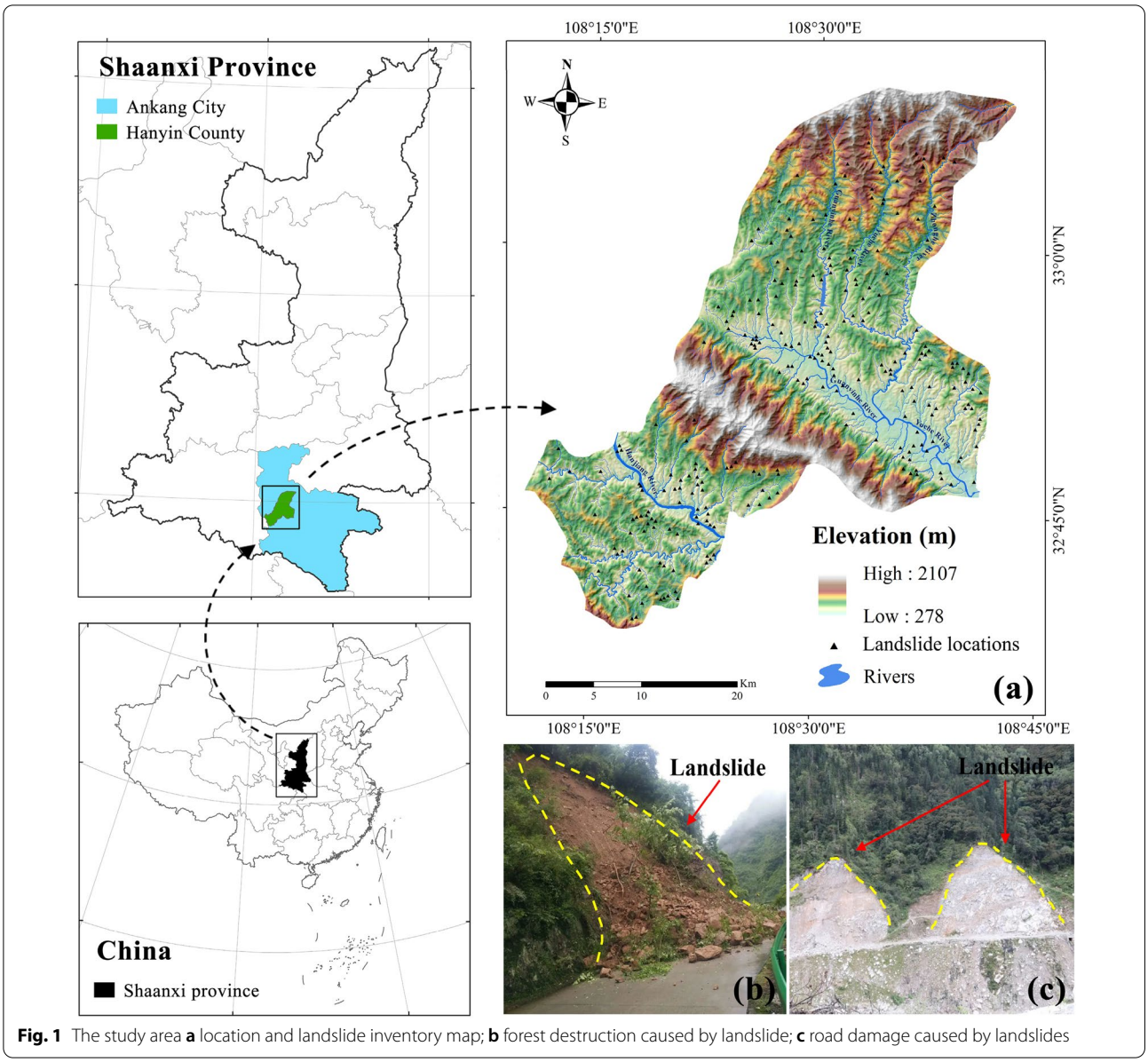

Fig. 1 The study area **a** location and landslide inventory map; **b** forest destruction caused by landslide; **c** road damage caused by landslides

Table 1 The main lithology information of the study area

Geological age	Symbol	Main lithology
Quaternary	Q	Sandy clay, clay rock
Tertiary	E	Clay rock, siltstone, glutenite
Middle Devonian	D_2	Limestone, calcium schist
Lower Devonian	D_1	Calcium schist, calcium sandstone, granite
Silurian	S	Phyllite and siliceous rock, sandstone
Ordovician	O	Argillaceous limestone, carbonaceous schist, quartzite
Cambrian	Є	Limestone, slate, phyllite
Senian	Z	Limestone, quartzite, schist

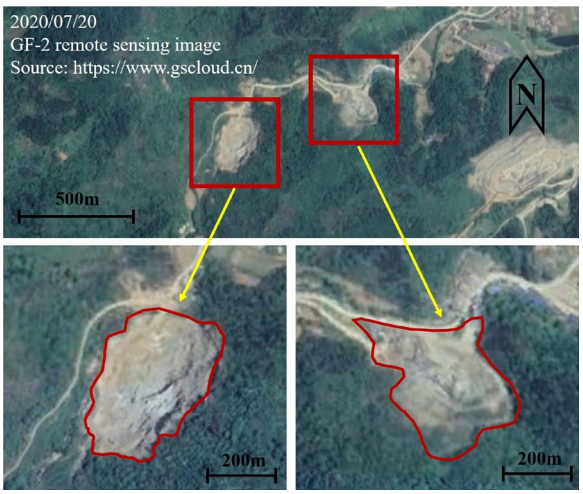

Fig. 2 The preparation process of landslide inventory map

coverage. Positive value expresses that the earth coverage is vegetation, and the larger the coverage extent of the vegetation lead to higher NDVI positive value.

At present, it is generally believed that the mechanism of landslide occurrence is the increase of pore water pressure in slope compositions by using the rainwater infiltration and accumulation during the rainy period. The high pore water pressure will lead to the increase of the effective load stress and the decrease of the shear strength of slope components, which are main triggering factors caused landslide. Therefore, MAP also occupies vital status of the landslide occurrence.

Rivers can affect the hydrogeology characteristics of slopes, and rivers usually corrode the toe of slope, which may decrease the anti-slide force. In mountainous area, it is common that numerous of landslide hazards are triggered by road constructions. Besides, in areas with frequent tectonic movements, the dislocation of faults can also cause landslide occurrence. Hence, distance to rivers, distance to roads, and distance to faults were regarded as predisposing factors in this study.

The lithology of the slope is the material foundation of the landslide. Some slopes are made up of hard rocks, some of which are made up of soft rocks, and some of them are made up of soil. Because of the difference between the lithologies, their shear strength varies. Often, slopes made of hard rocks do not easily fall, while slopes material of soft rocks or soil are easier to be destabilization deformation.

Since the original attribute data of each predisposing factor are very different, the frequency ratio (FR) is introduced to unify the dimension of each predisposing factor. The calculation process of FR value is shown in Eq. (1):

$$\mathrm{FR} = {}^{\mathrm{Sam_{ij}}}/_{\mathrm{Are_{ij}}}, \tag{1}$$

where $\mathrm{Sam_{ij}}$ stands for the percentage of landslides in each landslide predisposing factor class, and $\mathrm{Are_{ij}}$ is the area percentage of each landslide predisposing factor class (Siahkamari et al. 2017).

Additionally, in order to calculate the FR value, it is necessary to classify the predisposing factors, and the data sources, resolution and classification method of each predisposing factor are listed in Table 2.

Methodologies

The main research contents include 4 parts: (1) using the data that are already available to complete the landslide inventory; (2) using FR value to quantify the landslide

Table 2 The information and data source of landslide predisposing factors

Landslide predisposing factors	Original format	Resolution	Classification method	Data source
Altitude (m)	Grid	30 m × 30 m	natural break (Jenks)	Extracting from DEM image (http://www.gscloud.cn/)
Slope angle (°)	Grid	30 m × 30 m	natural break (Jenks)	Extracting from DEM image (http://www.gscloud.cn/)
Slope aspect	Grid	30 m × 30 m	natural break (Jenks)	Extracting from DEM image (http://www.gscloud.cn/)
NDVI	Grid	30 m × 30 m	natural break (Jenks)	Generating by GF-2 remote sensing images obtained from Xi'an Satellite Measurement and Control Center
Distance to rivers (m)	Vector	30 m × 30 m	Equal interval	Generating by regional water system obtained from the local government
Distance to roads (m)	Vector	30 m × 30 m	Equal interval	Generating by regional traffic maps obtained from the local government
Distance to faults (m)	Vector	30 m × 30 m	Equal interval	Extracting from geological maps with 1:500,000 scale obtained from the local government
MAP (mm/year)	Vector	30 m × 30 m	Equal interval	Extracting from rainfall observation data from 2010 to 2021 obtained from the local government
Lithology	Vector	30 m × 30 m	Custom interval	Extracting from geological maps with 1:500,000 scale obtained from the local government

predisposing factor maps, and partitioning dataset; (3) using the factor maps that are already quantified by FR to train the SVM model and KLR model, moreover using the original factor maps to train the LSNet model; (4) producing LSM corresponding to each model, assessing the result accuracy, and comparing the prediction performance of each model. The flowchart of this study is shown in Fig. 3. The techniques used in this study are described as follows.

Factor optimization method

Since the assumption of machine learning modeling is that the variables are independent of each other, it needs to detect whether there is strong correlation between the factors. This strong correlation relationship is called multicollinearity which may cause the over-fitting or under-fitting problems (Hong et al. 2018). In this study, the variance inflation factor (VIF) and tolerances (TOL) were applied to reflect the multicollinearity problem, which can be calculated by constructing a linear regression model based on the training dataset. When VIF > 10 and TOL < 0.1, it indicates that the predisposing factor has a multicollinearity problem and needs to be eliminated, vice versa (Pham et al. 2019).

Support vector machine model (SVM)

The basic principle of SVM is to search the optimal separating hyperplane that can maximize the interval between positive and negative samples in training dataset (Wang and Brenning 2021). Initially, SVM model was used as the supervised learning algorithm to solve binary classification problem, while the non-linear classification problem can be solved after introducing the kernel function. Therefore, the SVM model was applied in many researches about landside susceptibility assessment. In addition, there are three parameters namely penalty factor (C_0), non-sensitive loss function (ε), and kernel function parameter (γ) that need to be adjusted appropriately in the process of constructing the SVM model (Xie et al. 2021). The main steps of SVM model construction can be described as below.

At first, the landslide predisposing factors are defined as the dataset of instance label pairs (s_i, t_i, i = 1, 2, …, n), where s_i stands for the input data, t_i is the output classes (landslide and non-landslide), and n is the number of training samples (Kumar et al. 2017). The training samples are mapped in to a n-dimensional hyperplane by using the RBF kernel function which can be defined as:

$$K(s_i, s_j) = \left(-\gamma\left(s_i - s_j\right)\right), \gamma > 0. \tag{2}$$

Then mathematical expression of the n-dimensional hyperplane L needs to satisfy the following condition:

$$t_j\left(w \cdot s_j + b\right) + \varepsilon \geq 1, \tag{3}$$

where w denotes for the norm of normal hyperplane, and b is the constant. The maximum interval between vector and hyperplane can be derived by applying the

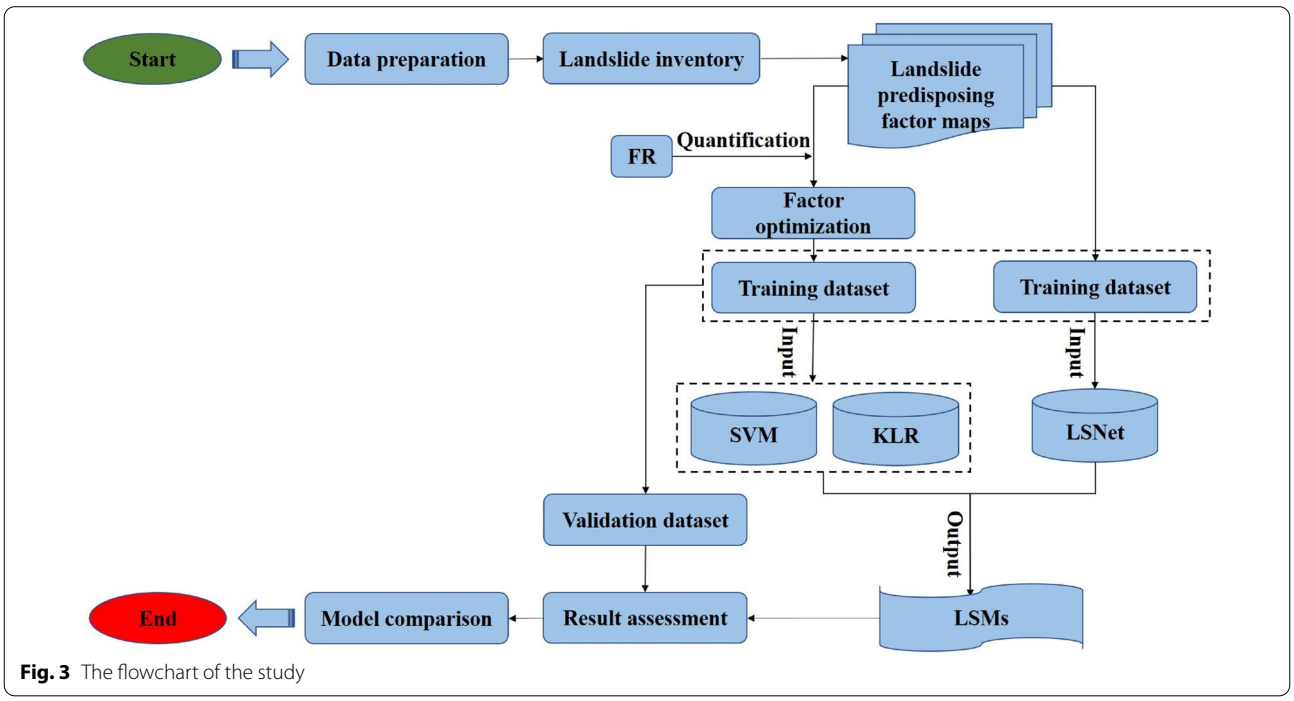

Fig. 3 The flowchart of the study

Lagrangian multiplier (Abedini et al. 2019), and cost function can be expressed as:

$$L = 1/2w^2 - C_0 \sum_{i=1}^{n} \varepsilon. \tag{4}$$

Kernel logistic regression model (KLR)

In statistical learning, when there are phenomena such as non-linear estimation, non-normal estimation, and uneven variance, it may cause invalid estimation by using the ordinary regression method (Chen et al. 2018). These problems were overcome after the introduction of logistic regression, and logistic regression is widely used to solve binary classification problem. However, the structure of original logistic regression model is relatively simple, the flexibility is relatively low, and it still has defects in dealing with non-linear classification problems (Chen et al. 2019). While the kernel function can help to solve these problems effectively in constructing logistic regression model. Therefore, the hybrid model, namely kernel logistic regression is created. In order to be consistent with the SVM model above, the RBF kernel function is determined to build KLR model. The expression of KLR model is as follows:

$$p_i(t = 1|k_i) = \frac{1}{1 + e^{-(k_i+\alpha)}}, \tag{5}$$

where p_i is the probability of landslide occurrence, k_i stands for the i th row of $K(s_i, s_j)$, and α is a constant for the intercept (Thai and Indra 2018).

Landslide net model (LSNet)

The deep learning has been widely used in the field of remote sensing image processing, including change detection, land use classification, image registration and so on. The deep belief networks, convolutional neural network (CNN), and auto coder are the three most commonly used network models in deep learning. The operating principle of these networks is to stack multiple layers within the model, and use the output of the previous item as the input of the next item, so that the features of each layer in the network can be converted into higher-dimensional features (Bui et al. 2020). Among them, the CNN has robust feature extraction capabilities and has been successfully applied in the field of image processing.

LSNet is a multi-layer feedforward neural network, the advantage of which is that it can process large-scale data in the form of multiple arrays from the local and global input data. The structure of LSNet is consist of multiple layers, which are related to each other through a set of learnable weights and biases. The local and global-scale features can be captured by these convolutional blocks using scanning of the entire image. Meanwhile, the pooling layer and rectified linear unit (ReLU) layer are used for generalization to improve the non-linear fitting ability of the network (Li et al. 2021). Additionally, each convolutional layer contains feature maps obtained by multiple convolution kernels, and these feature maps share the node weights of the convolution kernels, so features can be extracted from different parts (Fig. 4). Specifically, the main operation performing in CNN can be generalized as follows:

$$O^l = pool_p\left(\sigma\left(O^{l-1} * W^l + b^l\right)\right), \tag{6}$$

where O^{l-1}denotes the input feature map in lth layer, W^l and b^l, respectively, represent the weight and deviation of input feature layer convoluting by linear convolution, and σ is a non-linear function outside the convolution layer.

Assessment and comparison method

Result assessment method

In order to assess the accuracy of classification result and compare the performance of each model, statistical indexes are purposed to finish this work. A matrix (Table 3) is constructed by true positive (TP), false positive (FP), true negative (TN), and false negative (FN) calculating from training dataset (Pham et al. 2021). The accuracy and precision are calculated according to Eqs. (7) and (8) for accuracy assessment, meanwhile, the consistency of the results is verified with F1. The calculation process is as follows:

$$Accuracy = \frac{TP + TN}{TP + TN + FP + FN}, \tag{7}$$

$$Precision = \frac{TP}{TP + FP}, \tag{8}$$

$$1 = \frac{2 * precision * \frac{TP}{TP+FN}}{precision + \frac{TP}{TP+FN}}. \tag{9}$$

Model comparison method

In this study, the work of model comparison is purposed to carry out from three indicators including the running speed of the model, the classification ability for landslide and non-landslide, and the generalized performance of the model. Among them, based on the validation dataset, the running speed of the model is quantitative expressed by time, and the sensitivity and specificity are, respectively, used to reflect the classification ability for landslide and non-landslide (Eqs. (9) and (10)) (Yanar et al. 2020). Additionally, the receiver operating characteristics curve

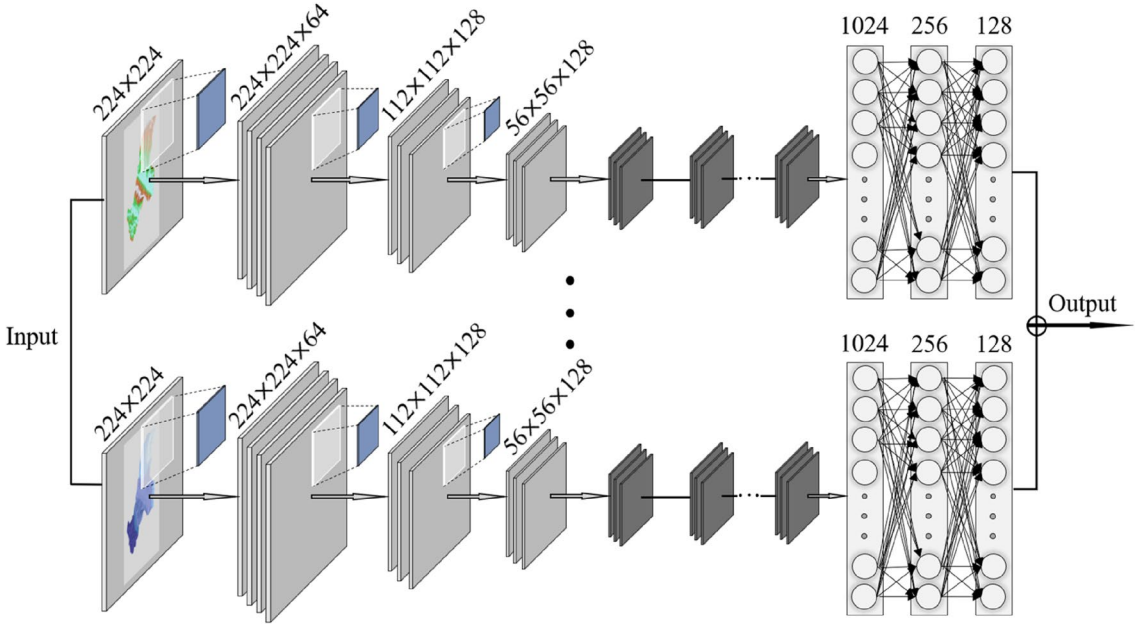

Fig. 4 The structure schematic diagram of landslide net (LSNet)

Table 3 Discriminant matrix of statistical indexes

Samples		Predicted label	
		Landslide	Non-landslide
True label	Landslide	True positive (TP)	True negative (TN)
	Non-landslide	False positive (FP)	False negative (FN)

(ROC) is used for assessing the generalized performance, and in general, the larger the area under ROC curve (AUROC), the stronger the generalization ability of the model (Dang et al. 2020):

$$Sensitivtiy = \frac{TP}{TP + FN}, \tag{10}$$

$$Specificity = \frac{TN}{TN + FP}. \tag{11}$$

Results

The quantification results of FR for landslide predisposing factors

In this study, the FR value was employed to quantify each landslide predisposing factor according to the classification result. It can be observed from Table 4 that the interval of Tertiary from the lithology factor has the highest FR value (FR = 2.32), followed by the range of < 100 from the distance to roads factor (FR = 1.85), and the range of 278–548 from the altitude factor (FR = 1.81). On the contrary, the lowest FR value appears in both the 1432–2107 interval of the altitude factor (FR = 0.00) and the flat interval of the slope factor (FR = 0.00).

The optimization result of landslide predisposing factors

The VIF and TOL values of each landslide predisposing factor were calculated based on the quantified landslide predisposing factors, and the calculation results are shown in Table 5. As can be seen from the results, the largest VIF value and the smallest TOL value appear in NDVI (VIF = 1.433, TOL = 0.698), followed by the altitude (VIF = 1.293, TOL = 0.773) and the aspect (VIF = 1.268, TOL = 0.789). By contrast, the distance to roads has the smallest VIF value and the largest TOL value (VIF = 1.019, TOL = 0.981). Since the VIF and TOL values of all landslide predisposing factors are not inside the critical range (VIF > 10 and TOL < 0.1), all factors are retained and used to prepare the dataset.

Based on the optimized landslide predisposing factors, the training and validation datasets were prepared according to aforementioned partition principle. Subsequently, the training dataset was used as the input data to implement the following three models.

Implementation of SVM model

In this study, the training dataset was used to construct the SVM model. Since the parameters of RBF kernel function are significant for model construction, the

Table 4 The FR calculation result for each class of landslide predisposing factors

Landslide predisposing factors	Classes	Are_{ij} (%)	Sam_{ij} (%)	FR
Altitude (m)	278–548	32.00	57.98	1.81
	548–781	31.06	28.02	0.90
	781–1075	17.68	11.67	0.66
	1075–1432	12.33	2.33	0.19
	1432–2107	6.93	0.00	0.00
Slope angle (°)	0.0000–9.6093	19.68	30.35	1.54
	9.6093–17.3502	27.24	31.91	1.17
	17.3502–24.8241	26.64	24.12	0.91
	24.8241–33.6327	18.95	10.51	0.55
	33.6327–67.7992	7.49	3.11	0.42
Slope aspect	Flat	0.06	0.00	0.00
	North	10.71	8.17	0.76
	Northeast	11.81	11.28	0.96
	East	15.32	19.84	1.30
	Southeast	12.82	12.84	1.00
	South	11.01	14.01	1.27
	Southwest	11.43	7.78	0.68
	West	14.37	16.34	1.14
	Northwest	12.47	9.73	0.78
NDVI	−0.0983–0.1717	7.26	5.45	0.75
	0.1717–0.2410	19.94	12.06	0.60
	0.2410–0.3030	28.86	31.13	1.08
	0.3030–0.3698	28.81	35.02	1.22
	0.3698–0.5308	15.13	16.34	1.08
Distance to rivers (m)	< 100	7.19	8.56	1.19
	100–200	5.48	6.23	1.14
	200–300	5.16	7.39	1.43
	300–400	4.94	7.78	1.57
	> 400	77.22	70.04	0.91
Distance to roads (m)	< 100	6.30	11.67	1.85
	100–200	5.39	8.17	1.51
	200–300	4.82	7.78	1.62
	300–400	4.50	6.23	1.38
	> 400	79.00	66.15	0.84
Distance to faults (m)	< 1000	11.60	19.46	1.68
	1000–2000	10.87	12.84	1.18
	2000–3000	9.77	11.67	1.19
	3000–4000	8.88	9.73	1.10
	> 4000	58.87	46.30	0.79
Lithology	Quaternary	18.02	28.40	1.58
	Tertiary	3.69	8.56	2.32
	Middle Devonian	9.46	1.95	0.21
	Lower Devonian	2.40	1.95	0.81
	Silurian	4.49	1.95	0.43
	Ordovician	2.38	1.17	0.49
	Cambrian	25.54	14.40	0.56
	Senian	33.99	36.19	1.06

Table 4 (continued)

Landslide predisposing factors	Classes	Are_{ij} (%)	Sam_{ij} (%)	FR
MAP (mm/year)	< 800	12.03	7.39	0.61
	800–850	22.39	19.84	0.89
	850–900	31.01	39.69	1.28
	900–950	14.82	10.12	0.68
	950–1000	3.37	5.06	1.50
	> 1000	16.39	17.90	1.09

Table 5 The VIF and TOL values of each landslide predisposing factor

Landslide predisposing factors	VIF	Tolerances (TOL)
Altitude	1.293	0.773
Slope angle	1.032	0.969
Aspect	1.268	0.789
MAP	1.044	0.958
Lithology	1.103	0.907
Distance to rivers	1.148	0.871
Distance to faults	1.078	0.928
Distance to roads	1.019	0.981
NDVI	1.433	0.698

tenfold cross-validation method was used to search the most suitable parameter set (C_0,γ). The optimized parameter set is (241, 0.02). Then run the trained SVM model in the python platform, and adjust the output range of the model to 0.000–1.000 which also represents the LSI. In the end, the natural break (Jenks) method was used to divide the LSI into five ranges which, respectively, represent the very low susceptibility area (0.0899–0.2084), low susceptibility area (0.2085–0.4646), moderate susceptibility area (0.4647–0.6228), high susceptibility area (0.6229–0.7893) and very high susceptibility area (0.7894–0.9224), furthermore the LSM was generated by converting these areas to image in ArcGIS software (Fig. 5).

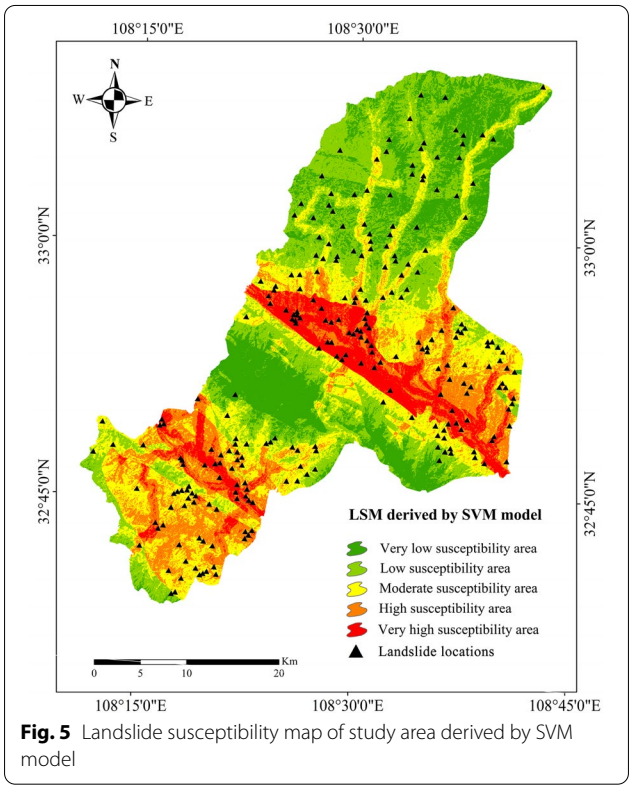

Fig. 5 Landslide susceptibility map of study area derived by SVM model

Implementation of KLR model

The construction progress of KLR model is similar to the SVM model. For the purpose of comparison, the parameter set (C_0,γ) was consistent with that of the SVM model. Subsequently, the training dataset was used as the input data for KLR model construction in the python platform, and the output range of the LSI was adjusted to 0.000–1.000. Finally, the LSI was divided into five ranges by using the natural break (Jenks) method. These five ranges, respectively, represent the very low susceptibility area (0.0145–0.2459), low susceptibility area (0.2460–0.3695), moderate susceptibility area (0.3696–0.5161), high susceptibility area (0.5162–0.6974) and very high susceptibility area (0.6975–0.9983), moreover the LSM corresponding to KLR model was generated in ArcGIS software (Fig. 6).

Implementation of LSNet model

The LSNet was coded using tensorflow 2.0 under the python environment, and running on a personal computer with Intel(R) Core(TM) i7-7700 k CPU, RTX 3080Ti GPU, 32 GB RAM, and the Windows 10 operating system. The LSNet had multi-layer structure, the size of input window was designed as 224×224. In fact, many researchers in image processing have

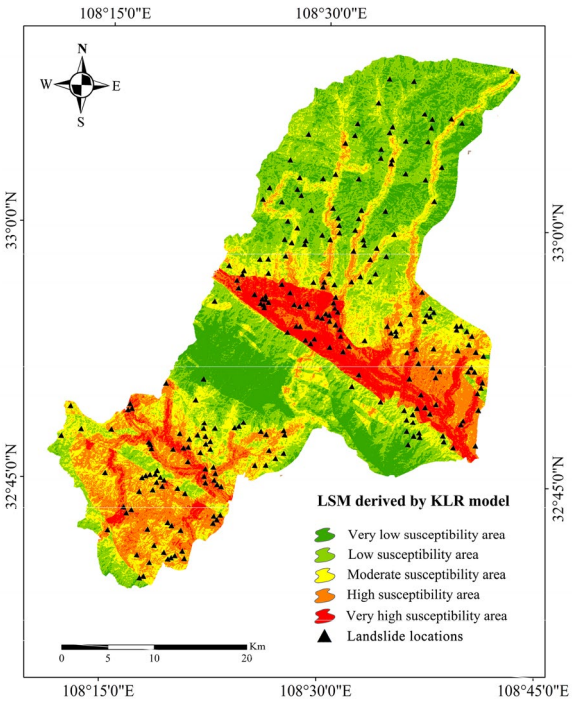

Fig. 6 Landslide susceptibility map of study area derived by KLR model

demonstrated that the size of the data input has little effect on the task objective. Based on the data of multiple channels we input, the data size of 224 has already covered the entire area of Hanyin County. In theory, the context relationship of this range can fully meet the needs of LSA. In addition, we also used 96, 128, 196, 224, 256 image blocks to conduct experiments, respectively. The results show that the size of the input data has no obvious effect on the test accuracy.

AlexNet can implement more than 1000 categories of classification. In contrast, the landslide susceptibility mapping is a binary classification problem, which does not require deep network design. For this reason, in this study, the size of input layer in convolution kernel of LSNet was set to 5×5, the size of the convolution kernel for the other layers was set to 3×3, the number of feature maps for each layer was set to 64, 128, 128, 256, 256, respectively. At the same time, a pooling layer, non-linear activation function ReLU and batch normalized BN were set after each convolutional layer. Based on computer graphics vision, all other parameters of the LSNet were empirically optimized, for instance, the learning rate and epoch are set as 0.0001 and 600 to learn the depth features through back propagation. Subsequently, the number of neurons in the fully connected layers was set to 1024, 256, 128, 2, respectively (Table 6). Since the classical network, VGG and UNet have proved the validity of 3×3 convolution kernel and 64,128,256,1024 feature image parameters in various regression and classification tasks. Therefore, on the basis of these parameters, we design a network structure with multiple channel inputs and fuse them at the end of the network. In particular, we use the hyperparameter search method to obtain the fully connected layers and training parameters of the multi-channel fusion structure, such as learning rate, batch size and epoch. Finally, softmax was used to estimate the probability of landslide occurrence to output confidence, namely LSI.

Table 6 The architecture of LSNet

Layer	Feature map	Feature map	Size	Kernel Size	Stride	Activate
Input			224 × 224 × 3			ReLU
1	2 × CNN	64	224 × 224 × 64	3 × 3	1	ReLU
	Max pooling	64	112 × 112 × 64	3 × 3	2	ReLU
2	2 × CNN	128	112 × 112 × 128	3 × 3	1	ReLU
	Max pooling	128	56 × 56 × 128	3 × 3	2	ReLU
3	2 × CNN	256	56 × 56 × 256	3 × 3	1	ReLU
	Max pooling	256	28 × 28 × 256	3 × 3	2	ReLU
4	2 × CNN	512	28 × 28 × 512	3 × 3	1	ReLU
	Max pooling	512	14 × 14 × 512	3 × 3	2	ReLU
5	2 × CNN	512	14 × 14 × 512	3 × 3	1	ReLU
	Max pooling	512	7 × 7 × 512	3 × 3	2	ReLU
6	FC	–	25,088	–	–	ReLU
7	FC	–	1024	–	–	ReLU
8	FC	–	256	–	–	ReLU
9	FC	–	128	–	–	SoftMax

Similarly, the output range of LSI for LSNet was adjusted to 0.000–1.000, and, respectively, represents the very low susceptibility area (0.0045–0.2021), low susceptibility area (0.2022–0.3458), moderate susceptibility area (0.3459–0.4814), high susceptibility area (0.4815–0.8033) and very high susceptibility area (0.8034–0.9972) (Fig. 7).

Assessment of the results

The result of accuracy assessment

After mapping the LSMs of these three models, it is necessary to assess the quality of results. In this study, the matrix has been organized based on the validation dataset, then the accuracy, precision, and F1 values for each LSM were calculated (Table 7). As shown in Table 7, the LSNet model gets the highest accuracy value and precision value (accuracy = 0.950, precision = 0.951), by contrast, the SVM model gets the lowest accuracy value and precision value (accuracy = 0.825, precision = 0.850), while the performance of the KLR model is moderate. From the value of F1, the LSNet also gets the highest value (F1 = 0.951), followed by the KLR model and SVM model, which is also consistent with the ordering of accuracy and precision values.

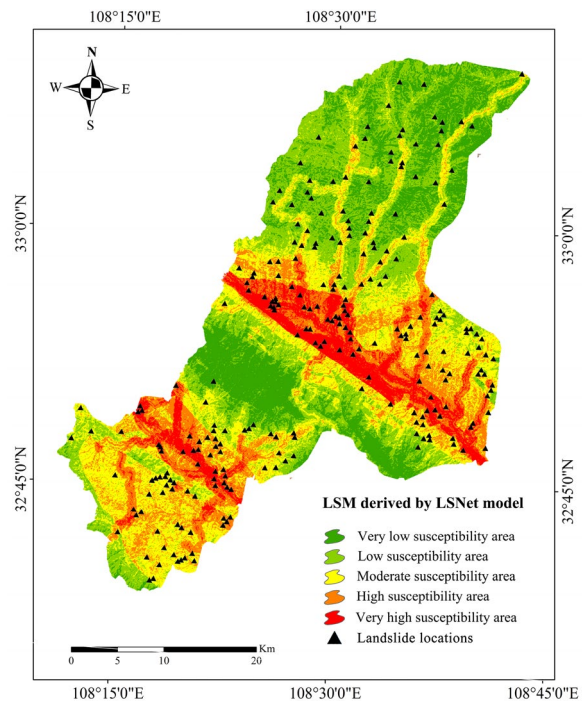

Fig. 7 Landslide susceptibility map of study area derived by LSNet model

Table 7 Calculation results of statistical indexes for landslide susceptibility mapping

Parameters	SVM	KLR	LSNet
TP	34	36	39
TN	32	36	37
FP	6	6	2
FN	8	2	2
Accuracy	0.825	0.900	0.950
Precision	0.850	0.857	0.951
F1	0.829	0.900	0.951
Sensitivity	0.810	0.947	0.951
Specificity	0.842	0.857	0.949

The result of model comparison

In order to compare the running speed, classification and generalization performance, the run time, sensitivity, specificity and AUROC values were introduced to finish this work. As the results shown in Table 7, the largest sensitivity and specificity values belong to the LSNet model, indicating that the LSNet model has the best landslide and non-landslide classification abilities among these three models. On the contrary, the smallest sensitivity and specificity values belong to the SVM model, indicating that the landslide and non-landslide classification abilities of SVM model are the weakest among these three models.

For AUROC values (Fig. 8), the LSNet model also obtains the largest AUROC value (AUROC = 0.941), followed by the KLR model (AUROC = 0.899) and SVM model (AUROC = 0.835), and the results show that the LSNet model has the best generalization ability.

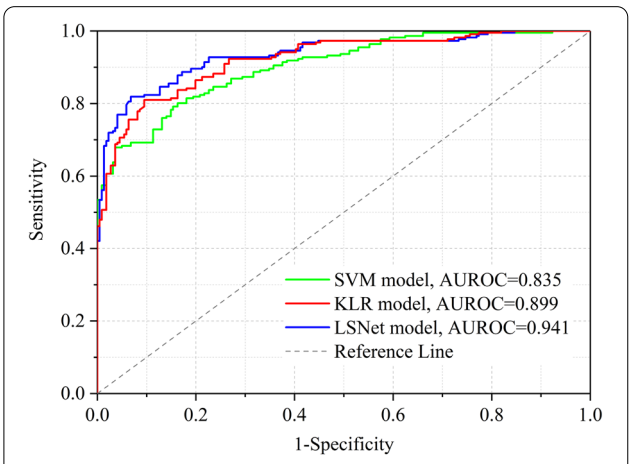

Fig. 8 The ROC curves of each landslide susceptibility model based on validation dataset

Lastly, we measured the running speed of each model, the results show that the running speed of the SVM model (32 s) and the KLR model (27 s) are relatively close, while the running speed of the LSNet model (107 s) is significantly slower than the first models.

Discussion

In this paper, we show the progress and results of landslide susceptibility mapping based on SVM model, KLR model, and LSNet model in Hanyin County, Shaanxi Province, China. In terms of the model performance, although the classification accuracy of the three models is higher, the accuracy of LSNet and other statistical indexes are higher than that of SVM and KLR, which fully shows that the LSNet performs best in the study area.

Since both SVM and KLR are developed based on statistical theory, the quality of input data and the adjustment of model parameters in the process of model construction may affect the final result. Before preparation of input datasets, three classification methods, i.e., natural break (Jenks), equal interval, and custom interval were all used to grade FR-quantified landslide predisposing factors. However, the classification methods and results of landslide predisposing factors are inevitably affected by human factors, which may lead to over-fitting or under-fitting (Yacine and Pourghasemi 2019). For this reason, it is necessary to deeply analyze the impact of classification methods on data quality. Besides, this study only used two machine learning models for comparison, therefore, more models should be added for reference in subsequent research, so that the advantages and disadvantages of deep learning and machine learning in landslide susceptibility mapping can be more comprehensively compared.

In contrast, as a deep learning model, the input data of LSNet is a complete remote sensing image containing all the information. In order to distinguish landslide and non-landslide from image data, not only the objects in the image patch need to be characterized as landslides, but also need to accurately and reliably represent the contextual information of the landslide space background. The advantage of LSNet is to derive the category of the object at the image block level, and learn the spatial distribution through the CNN network with hierarchical representation, and finally obtain the probability of each object's category through multiple fully connected layers and softmax. It is different from machine learning in principle, and its specific advantages include: (1) LSNet can classify based on object blocks in a deep learning network of convolutional structure, and output the category probability; (2) LSNet uses the CNN model to learn the internal and overall spatial information of the object block to represent the contextual spatial semantic information of the category. LSNet represents the probability of the category at the object block level, which can avoid pixel-level misfits and improve the accuracy of classification (Dimililer et al. 2021). (3) LSNet can directly read remote sensing images without destroying the data structure, and can obtain richer and multi-source data sets, making the trained model robust. Interestingly, the running time of LSNet is significantly longer than that of SVM and KLR, which may be limited by the hardware performance of the computer, resulting in slower calculations. Nevertheless, this does not mean that the LSNet is not a state-of-the-art model and other studies have reached similar conclusions in their researches. However, since the occurrence of landslides is affected by multi-source factors, the characteristics of the landslides themselves are also very complex and cannot be described solely by human-represented features. Therefore, we try our best to use deep learning methods that are completely data-driven. In addition, in this study, the final network architecture of LSNet was determined by gradually increasing the ablation experiments, and at the same time, an LSNet with multiple channels was established combined with the data structure representing the landslide, which could well fulfill the requirements of LSA. Furthermore, because other network structures are generated based on their respective research objects and purposes, although we cannot conduct experiments on these networks one by one, we have designed a network structure that matches the confidence of the current landslide research. We have also demonstrated the effectiveness and accuracy of LSNet in our experiments.

On the other hand, as a black box model, DL cannot intuitively reflect the spatial distribution features of landslides in the study area during data preparation. On the contrary, in machine learning modeling, because FR is used to quantify the graded landslide predisposing factors, the spatial distribution of the landslide under the conditions of each predisposing factor can be intuitively reflected from the quantified results (Zhang et al. 2020). For instance, from the view of distance to rivers and roads, as the distance from roads and rivers increase, the FR value decreases, indicating that the closer to the river and the road, the more landslides are distributed. This is because the exposed rock and soil in study area have low mechanical strength, the surface is easily weathered and eroded, and the joints and fissures are very developed. Moreover, due to the scouring action from the river and excavation of the slope toe during road construction, the original stress structure of the slope was destroyed, which resulted in the instability of the slope and generated a large number

of potential landslides. This consistent with the phenomenon we observed in the field, and is similar to the results of geological hazard studies in similar areas of the study area (Wang et al. 2016; Liu et al. 2020).

Conclusion

Landslide susceptibility mapping is a key step for landslide prevention work. This study used Hanyin County, Shaanxi Province, China as the study area to complete the work of landslide susceptibility mapping by building the LSNet model, SVM model, and KLR model, and generated the LSM. Then various statistical indexes were applied for the accuracy assessment, and the ROC curves was employed to compare the performance and classification ability of the models. In summary, the main conclusions are as follows: (1) in the process of dataset preparation and parameter adjustment, the machine learning model will inevitably be affected by human factors, resulting in unstable classification results. However, LSNet can overcome human interference and generate objective classification results. (2) LSNet can avoid the problems of over-fitting and under-fitting. The classification accuracy in the study area is high, moreover the generalization is stronger than the SVM model and the KLR model. The LSNet can be promoted and used in the study area.

This study introduced the construction method of LSNet model in detail, and compared the performance of LSNet model (deep learning), SVM model (machine learning), and KLR model (hybrid model), which enriched the landslide database of the study area and can provide reference for the application of deep learning model in landslide prevention in the future. Furthermore, the results of this study can improve the efficiency of landslide prevention for government decision-making in similar study areas, which is conducive to rapid response of landslide warning. Comprehensive risk assessors and land use planner can benefit from our study findings. Additionally, the proposed approach is an innovative method that may also help other scientists to develop landslide susceptibility maps in other areas, but also as an approach that could be used in geo-environmental problems besides natural hazard assessments.

Acknowledgements
The authors wish to express their sincere thanks to Heng Zhang (Chang'an University) for useful information provided.

Author contributions
Conceptualization, TZ and HW; methodology, TC; software, DL; validation, TZ; formal analysis, ZS; investigation, LH; resources, CL; data curation, TW; writing—original draft preparation, TZ; writing—review and editing, TZ and HW; visualization, YL; supervision, LH; project administration, TZ; funding acquisition, TZ. All authors have read and agreed to the published version of the manuscript.

Funding
This study is financially supported by Shaanxi Province Natural Science Basic Research Program (2022JQ-457), National Natural Science Foundation of China (211035210511), Fundamental Research Funds for the Central Universities (300102351502), Shaanxi Province Enterprises Talent Innovation Striving to Support the Plan (2021–1-2–1), and Inner scientific research project of Shaanxi Land Engineering Construction Group (SXDJ2021-10, SXDJ2021-30, SXDJ2022-16).

Availability of data and materials
Restrictions apply to the availability of these data. Data were obtained from Hanyin County People's Government and are available http://www.hanyin.gov.cn/ with the permission of Hanyin People's Government.

Declarations

Competing interests
The authors declare no conflict of interest.

Author details
[1]Key Laboratory of Degraded and Unused Land Consolidation Engineering, the Ministry of Natural Resources, Xi'an, Shaanxi, China. [2]Institute of Land Engineering and Technology, Shaanxi Provincial Land Engineering Construction Group Co., Ltd, Xi'an, Shaanxi, China. [3]Shaanxi Provincial Land Engineering Construction Group Land Survey Planning and Design Institute Co., Ltd, Xi'an, Shaanxi, China. [4]School of Land Engineering, Chang'an University, Xi'ani 710054, Shaanx, China.

Received: 15 July 2021 Accepted: 7 July 2022
Published online: 25 July 2022

References

Abedini M, Ghasemian B, Shirzadi A et al (2019) A comparative study of support vector machine and logistic model tree classifiers for shallow landslide susceptibility modeling. Environ Earth Sci 78:560–577. https://doi.org/10.1007/s12665-019-8562-z

Aditian A, Kubotab T, Shinoharab Y (2018) Comparison of GIS-based landslide susceptibility models using frequency ratio, logistic regression, and artificial neural network in a tertiary region of Ambon, Indonesia. Geomorphology 318:101–111. https://doi.org/10.1016/j.geomorph.2018.06.006

Aghdam IN, Pradhan B, Panahi M (2017) Landslide susceptibility assessment using a novel hybrid model of statistical bivariate methods (FR and WOE) and adaptive neuro-fuzzy inference system (ANFIS) at southern Zagros Mountains in Iran. Environ Earth Sci 76:237–255. https://doi.org/10.1007/s12665-017-6558-0

Balogun A-L, Rezaie F, Pham QB et al (2021) Spatial prediction of landslide susceptibility in western Serbia using hybrid support vector regression (SVR) with with GWO, BAT and COA algorithms. Geosci Front 12:101–104. https://doi.org/10.1016/j.gsf.2020.10.009

Benzekri W, Moussati AE, Moussaoui O et al (2020) Early forest fire detection system using wireless sensor network and deep learning. Int J Adv Comput Sci Appl 11:496–502. https://doi.org/10.14569/IJACSA.2020.0110564

Bui DT, Tuan TA, Klempe H et al (2016) Spatial prediction models for shallow landslide hazards: a comparative assessment of the efficacy of support vector machines, artificial neural networks, kernel logistic regression, and logistic model tree. Landslides 13:361–378. https://doi.org/10.1007/s10346-015-0557-6

Bui DT, Shahabi H, Shirzadi A et al (2018) Landslide detection and susceptibility mapping by AIRSAR data using support vector machine and index of entropy models in cameron highlands, Malaysia. Remote Sens 10:1527–1533. https://doi.org/10.3390/rs10101527

Bui T-A, Lee P-J, Lum K-Y et al (2020) Deep learning for landslide recognition in satellite architecture. IEEE Access PP. https://doi.org/10.1109/ACCESS.2020.3014305

Carranza EJM (2015) Data-driven evidential belief modeling of mineral potential using few prospects and evidence with missing values. Nat Resour Res 24:291–304. https://doi.org/10.1007/s11053-014-9250-z

Carrara A, Cardinali M, Guzzetti F et al (1995) Gis Technology in Mapping Landslide Hazard. Geogr Inform Sys Assess Nat Hazards 8:135–175. https://doi.org/10.1007/978-94-015-8404-3_8

Chen W, Shahabi H, Shirzadi A et al (2018) Novel hybrid artificial intelligence approach of bivariate statistical-methods-based kernel logistic regression classifier for landslide susceptibility modeling. Bull Eng Geol Env 78:4397–4419. https://doi.org/10.1007/s10064-018-1401-8

Chen W, Yan X, Zhao Z et al (2019) Spatial prediction of landslide susceptibility using data mining-based kernel logistic regression, naive Bayes and RBFNetwork models for the Long County area (China). Bull Eng Geol Env 78:247–266. https://doi.org/10.1007/s10064-018-1256-z

Chen W, Chen X, Peng J et al (2021) Landslide susceptibility modeling based on ANFIS with teaching-learning-based optimization and Satin bowerbird optimizer. Geosci Front 12:93–107. https://doi.org/10.1016/j.gsf.2020.07.012

Cloud GD (2020) (GF-2) PMS sub-meter high resolution data products, 2020, Retrieved August 10, 2020, http://www.gscloud.cn/sources/accessdata/421?pid=302

Conoscenti C, Ciaccio M, Caraballo-Arias NA et al (2014) Assessment of susceptibility to earth-flow landslide using logistic regression and multivariate adaptive regression splines: a case of the Bence River basin (western Sicily, Italy). Geomorphology 242:49–64. https://doi.org/10.1016/j.geomorph.2014.09.020

Constantin M, Bednarik M, Jurchescu MC et al (2011) Landslide susceptibility assessment using the bivariate statistical analysis and the index of entropy in the Sibiciu Basin (Romania). Environ Earth Sci 63:397–406. https://doi.org/10.1007/s12665-010-0724-y

Dang V-H, Hoang N-D, Nguyen L-M-D et al (2020) A novel GIS-based random forest machine algorithm for spatial prediction of shallow landslide susceptibility. Forests. https://doi.org/10.3390/f11010118

Dimililer K, Dindar H, Al-Turjman F (2021) Deep learning, machine learning and internet of things in geophysical engineering applications: an overview. Microprocess Microsyst 80:103–613. https://doi.org/10.1016/j.micpro.2020.103613

Fan W, Wei XS, Cao YB et al (2017) Landslide susceptibility assessment using the certainty factor and analytic hierarchy process. J Mt Sci 21:100–119. https://doi.org/10.1007/s11629-016-4068-2

Fang Z, Wang Y, Peng L et al (2021) A comparative study of heterogeneous ensemble learning techniques for landslide susceptibility mapping. Int J Geogr Inf Sci 35:321–347. https://doi.org/10.1080/13658816.2020.1808897

Guzzetti F, Mondini AC, Cardinali M et al (2012) Landslide inventory maps: new tools for an old problem. Earth Sci Rev 112:42–66. https://doi.org/10.1016/j.earscirev.2012.02.001

Hong H, Liu J, Bui DT et al (2018) Landslide susceptibility mapping using J48 decision tree with adaboost, bagging and rotation forest ensembles in the Guangchang area (China). CATENA 163:399–413. https://doi.org/10.1016/j.catena.2018.01.005

Huang F, Zhang J, Zhou C et al (2020) A deep learning algorithm using a fully connected sparse autoencoder neural network for landslide susceptibility prediction. Landslides 17:217–229. https://doi.org/10.1007/s10346-019-01274-9

Kayastha P, Dhital MR, Smedt FD (2013) Application of the analytical hierarchy process (AHP) for landslide susceptibility mapping: a case study from the Tinau watershed, west Nepal. Comput Geosci 52:398–408. https://doi.org/10.1016/j.cageo.2012.11.003

Kumar D, Thakur M, S. Dubey C, et al (2017) Landslide susceptibility mapping & prediction using support vector machine for Mandakini River Basin, Garhwal Himalaya, India. Geomorphology 295:115–125. https://doi.org/10.1016/j.geomorph.2017.06.013

Kumar D, Roshni T, Singh A et al (2020) Predicting groundwater depth fluctuations using deep learning, extreme learning machine and gaussian process: a comparative study. Earth Sci Inf 13:1–14. https://doi.org/10.1007/s12145-020-00508-y

Li R, Wang N (2019) Landslide susceptibility mapping for the Muchuan County (China): a comparison between bivariate statistical models (WoE, EBF, and IoE) and their ensembles with logistic regression. Symmetry 11:762–781. https://doi.org/10.3390/sym11060762

Li J, Zhang Y (2017) GIS-supported certainty factor (CF) models for assessment of geothermal potential: a case study of Tengchong County, southwest China. Energy 140:552–565. https://doi.org/10.1016/j.energy.2017.09.012

Li W, Fang Z, Wang Y (2021) Stacking ensemble of deep learning methods for landslide susceptibility mapping in the three gorges reservoir area China. Environmental Res Risk Assess. https://doi.org/10.1007/s00477-021-02032-x

Liu Y, Huang Q (2006) The formation and mechanism of an expansive soil highway landslide. Coal Geol Explor 13:41–44. https://doi.org/10.1016/S1872-2040(06)60004-2

Liu H, Li X, Meng T et al (2020) Susceptibility mapping of damming landslide based on slope unit using frequency ratio model. Arab J Geosci 13:178–192. https://doi.org/10.1007/s12517-020-05689-w

Panahi M, Jaafari A, Shirzadi A et al (2020) Deep Learning Neural Networks for Spatially Explicit Prediction of Flash Flood Probability. Geosci Front 12:370–383. https://doi.org/10.1016/j.gsf.2020.09.007

Pandey VK, Pourghasemi HR (2020) Landslide susceptibility mapping using maximum entropy and support vector machine models along the highway corridor, Garhwal Himalaya. Geocarto Int 35:168–187. https://doi.org/10.1080/10106049.2018.1510038

Pham BT, Bui DT, Dholakia MB et al (2016) A Comparative Study of Least Square Support Vector Machines and Multiclass Alternating Decision Trees for Spatial Prediction of Rainfall-Induced Landslides in a Tropical Cyclones Area. Geotech Geol Eng 34:1807–1864. https://doi.org/10.1007/s10706-016-9990-0

Pham BT, Prakash I, K. Singh S, et al (2019) Landslide susceptibility modeling using reduced error pruning trees and different ensemble techniques: Hybrid machine learning approaches. CATENA 175:203–218. https://doi.org/10.1016/j.catena.2018.12.018

Pham QB, Yacine A, Ali SA et al (2021) A comparison among fuzzy multi-criteria decision making, bivariate, multivariate and machine learning models in landslide susceptibility mapping. Geomat Nat Haz Risk 12:1741–1777. https://doi.org/10.1080/19475705.2021.1944330

Polykretis C, Chalkias C (2018) Comparison and evaluation of landslide susceptibility maps obtained from weight of evidence, logistic regression, and artificial neural network models. Nat Hazards 93:249–274. https://doi.org/10.1007/s11069-018-3299-7

Pourghasemi HR, Moradi HR, Aghda SMF (2013) Landslide susceptibility mapping by binary logistic regression, analytical hierarchy process, and statistical index models and assessment of their performances. Nat Hazards 69:605–609. https://doi.org/10.1007/s11069-013-0728-5

Pradhan B, Lee S (2010) Delineation of landslide hazard areas on Penang Island, Malaysia, by using frequency ratio, logistic regression, and artificial neural network models. Environ Earth Sci 60:1037–1054. https://doi.org/10.1007/s12665-009-0245-8

PRC, 2020. The Ministry of emergency management released the basic situation of natural disasters nationwide in 2019. In, http://www.gov.cn/shuju/2020-01/17/content_5470130.htm (Accessd on 17 January 2020).

Razavizadeh S, Solaimani K, Massironi M et al (2017) Mapping landslide susceptibility with frequency ratio, statistical index, and weights of evidence models: a case study in northern Iran. Environ Earth Sci 76:499–512. https://doi.org/10.1007/s12665-017-6839-7

Saadoud D, Hassani M, Peinado FJM et al (2018) Application of fuzzy logic approach for wind erosion hazard mapping in Laghouat region (Algeria) using remote sensing and GIS. Aeol Res 32:23–24. https://doi.org/10.1016/j.aeolia.2018.01.002

Sameen MI, Pradhan B, Lee S (2020) Application of convolutional neural networks featuring Bayesian optimization for landslide susceptibility assessment. CATENA 186:104249. https://doi.org/10.1016/j.catena.2019.104249

SBGMR, 1989. Regional geology of shaanxi province. geological publishing house. (In Chinese), Bei Jing, China.

Siahkamari S, Haghizadeh A, Zeinivand H et al (2017) Spatial prediction of flood-susceptible areas using frequency ratio and maximum entropy models. Geocarto Int 33:927–941. https://doi.org/10.1080/10106049.2017.1316780

Soma AS, Kubota T, Mizuno H (2019) Optimization of causative factors using logistic regression and artificial neural network models for landslide susceptibility assessment in Ujung Loe Watershed, South Sulawesi Indonesia. J Mt Sci 16:144–162. https://doi.org/10.1007/s11629-018-4884-7

Sun X, Chen J, Han X et al (2020) Application of a GIS-based slope unit method for landslide susceptibility mapping along the rapidly uplifting section of the upper Jinsha River, South-Western China. Bull Eng Geol Env 79:533–549. https://doi.org/10.1007/s10064-019-01572-5

Thai PB, Indra P (2018) Machine learning methods of kernel logistic regression and classification and regression trees for landslide susceptibility assessment at part of Himalayan Area, India. Indian J Sci Technol 11:1–10. https://doi.org/10.17485/ijst/2018/v11i12/99745
Umar Z, Pradhan B, Ahmad A et al (2014) Earthquake induced landslide susceptibility mapping using an integrated ensemble frequency ratio and logistic regression models in West Sumatera Province, Indonesia. CATENA 118:124–135. https://doi.org/10.1016/j.catena.2014.02.005
Wang Z, Brenning A (2021) Active-learning approaches for landslide mapping using support vector machines. Remote Sens 13:2588–2607. https://doi.org/10.3390/rs13132588
Wang L, Guo M, Sawada K et al (2016) A comparative study of landslide susceptibility maps using logistic regression, frequency ratio, decision tree, weights of evidence and artificial neural network. Geosci J 20:117–136. https://doi.org/10.1007/s12303-015-0026-1
Wang Y, Fang Z, Hong H (2019) Comparison of convolutional neural networks for landslide susceptibility mapping in Yanshan County, China. Sci Total Environ 666:975–953. https://doi.org/10.1016/j.scitotenv.2019.02.263
Wang W, He Z, Han Z et al (2020) Mapping the susceptibility to landslides based on the deep belief network: a case study in Sichuan Province, China. Nat Hazards 103:3239–3261. https://doi.org/10.1007/s11069-020-04128-z
Wu R, Zhang Y, Guo C et al (2020) Landslide susceptibility assessment in mountainous area: a case study of Sichuan-Tibet railway, China. Environ Earth Sci 79:157–177. https://doi.org/10.1007/s12665-020-8878-8
Xiao L, Zhang Y, Peng G (2018) Landslide susceptibility assessment using integrated deep learning algorithm along the China-Nepal highway. Sensors 18:4436–4472. https://doi.org/10.3390/s18124436
Xie W, Nie W, Saffari P et al (2021) Landslide hazard assessment based on bayesian optimization-support vector machine in Nanping City, China. Nat Hazards 26:18–31. https://doi.org/10.1007/s11069-021-04862-y
Yacine A, Pourghasemi HR (2019) How do machine learning techniques help in increasing accuracy of landslide susceptibility maps? Geosci Front 11:328–345. https://doi.org/10.1016/j.gsf.2019.10.001
Yanar T, Kocaman S, Gokceoglu C (2020) Use of mamdani fuzzy algorithm for multi-hazard susceptibility assessment in a developing Urban Settlement (Mamak, Ankara, Turkey). Int J Geo-Inf 9:114–128. https://doi.org/10.3390/ijgi9020114
Youssef AM, Pourghasemi HR (2021) Landslide susceptibility mapping using machine learning algorithms and comparison of their performance at Abha Basin, Asir Region, Saudi Arabia. Geosci Front 12:639–655. https://doi.org/10.1016/j.gsf.2020.05.010
Youssef AM, Mohamed A-K, Biswajeet P (2015) Landslide susceptibility mapping at Al-Hasher area, Jizan (Saudi Arabia) using GIS-based frequency ratio and index of entropy models. Geosci J 19:113–134. https://doi.org/10.1007/s12303-014-0032-8
Zhang T, Han L, Han J et al (2019) Assessment of landslide susceptibility using integrated ensemble fractal dimension with kernel logistic regression model. Entropy 21:218–234. https://doi.org/10.3390/e21020218
Zhang Y, Lan H, Li L et al (2020) Optimizing the frequency ratio method for landslide susceptibility assessment: a case study of the caiyuan basin in the Southeast mountainous area of China. J Mt Sci 17:340–357. https://doi.org/10.1007/s11629-019-5702-6
Zhao X, Chen W (2020) Optimization of computational intelligence models for landslide susceptibility evaluation. Remote Sensing 12:2180–2200. https://doi.org/10.3390/rs12142180
Zhou S, Fang L (2015) Support vector machine modeling of earthquake-induced landslides susceptibility in central part of Sichuan province, China. Geoen Disasters 2:303–315. https://doi.org/10.1186/s40677-014-0006-1
Zhu L, Huang L, Fan L et al (2020) Landslide Susceptibility prediction modeling based on remote sensing and a novel deep learning algorithm of a cascade-parallel recurrent neural network. Sensors 20:1576–1591. https://doi.org/10.3390/s20061576

Publisher's Note